Convergent N^2-scaling iterative method of photoelectron diffraction and low-energy electron diffraction for ordered or disordered systems

Huasheng Wu and S. Y. Tong
Department of Physics, The University of Hong Kong, Hong Kong, China
(Received 22 September 1998)

We present results of a convergent iterative method of photoelectron diffraction and low-energy electron diffraction. The computation time of this method scales as N^2, where N is the dimension of the propagator matrix, rather than N^3 as in conventional Gaussian substitutional methods. We show that the Rehr-Albers separable-representation cluster approach or slab-type nonseparable methods can all be cast in this iterative form. The convergence of this method is demonstrated for different materials. With the substantial savings in computational time and no loss in numerical accuracy, this method will be very useful in future applications of multiple-scattering theory, particularly for systems either involving very large unit cells (200–700 atoms) or where no long-range order is present. [S0163-1829(99)04003-5]

Over the years, a major accomplishment in surface science is the formulation of accurate multiple-scattering theories for structural determination.[1,2] However, current multiple-scattering theories of low-energy electron diffraction (LEED) and photoelectron diffraction for systems with long-range order involve the solution of a matrix-vector equation of the form $\{\mathbf{I}-\mathbf{M}\}\mathbf{x}=\mathbf{y}$. Here, $\mathbf{M}$ is a (complex) square matrix of dimension N, $\mathbf{I}$ is a unit matrix of the same dimension, and $\mathbf{x}$,$\mathbf{y}$ are (complex) vectors of length N. The ''exact'' solution $\mathbf{x}=\{\mathbf{I}-\mathbf{M}\}^{-1}\mathbf{y}$ requires Gaussian reduction and back substitution. These steps scale as N^3 in computational time. Because the number of atoms n per unit cell appears in first order in the dimension, current slab-type multiple-scattering theories have computation times scaling as n^3. The most complicated system studied so far by slab multiple-scattering theory is the Si(111) 7×7 surface. Using symmetry, Tong *et al.*[3] reduced the 98 atoms in the surface double-layer unit cell to 24 atoms. Because of the cubic dependence on n, current slab multiple-scattering theories become impractical with $n>50$.

On the other hand, real surfaces and interfaces contain defects.[4,5] Many materials properties are affected or even dominated by defects. Examples of defect-controlled properties include the concentration of carriers in a semiconductor or the activity of a catalyst on a surface. Since it is never possible to prepare a perfect surface or interface, then defect structures must be studied and understood. Additionally, controlled defects provide fundamental properties in artificially grown materials; notable examples are the one-, two-, and three-dimensional quantum-well structures.

To characterize defect structures, it is often necessary to treat by multiple-scattering theory systems with over 300 atoms either as a supercell in a slab method or as an isolated cluster. The purpose of this paper is to present results of a convergent-iterative multiple-scattering method whose computation time scales as N^2 or less, rather than N^3. Our method is equally applicable to the slab approach or the cluster approach. One of the most widely used cluster methods is the separable-perturbation approach of Rehr and Albers.[6] In the original formulation, multiple-scattering paths are expanded in a perturbation series to finite order. In this formulation, the number of scattering paths increases exponentially as the multiple-scattering (MS) order increases. We show how the Rehr-Albers (RA) cluster method can be cast into solving a system of linear equations, analogous to that of the slab method. We solve the system of linear equations by a relaxation-iterative method.[7] In our method, multiple scattering is summed until numerical convergence to a preset accuracy is achieved and the computation time increasing linearly with the MS order. To demonstrate the application of the method, we present results for photoelectron diffraction spectra of Ni clusters with different sizes, and for slab calculations of LEED IV curves of the c (2×2) Au on Cu(001) system. In each case, the convergence of our method is demonstrated by comparing the results with those obtained by slower, conventional methods.

We first describe the treatment for a cluster. Following Rehr-Albers,[6] the photoelectron-diffraction intensity collected by a detector at $\vec{R}_d=\vec{R}_Q$ is

$$I(\vec{k})\propto\left|\sum_{L_f}\sum_{Q=1}^{\infty}\mathbf{G}^{(Q-1)}_{L_f,00}(\vec{R}_1,\vec{R}_2,\ldots,\vec{R}_Q=\vec{R}_d)m_{L_f}e^{i\delta_{l_f}}\right|^2\rho_d^2. \tag{1}$$

In Eq. (1), L_f denotes the photoexcitation dipole-element's final state, k_0 is the electron's wave number. The emitting atom is at $\vec{R}_0$ and the detector is at $\vec{R}_d=\vec{R}_Q\rightarrow\infty$. The master origin is located at the vacuum-solid interface. The matrix element from a core level to L_f is given by m_{L_f} and δ_{l_f} is a partial-wave phase shift. The MS order $(Q-1)$ denotes the number of scatterers (i.e., t matrices) in each scattering path. The vectors $\vec{\rho}_i=k_0$ $(\vec{R}_i-\vec{R}_{i-1})$. By introducing the RA separable representation of $\mathbf{G}_{L'L}(\vec{\rho})$, the total propagator for the $(Q-1)$th order can be written as

$$\mathbf{G}^{(Q-1)}_{L_f,00}(\vec{R}_1,\vec{R}_2,\ldots,\vec{R}_Q=\vec{R}_d)$$
$$=\sum_{\text{all paths}}\frac{e^{i(\rho_1+\rho_2+\cdots\rho_Q)}}{\rho_1\rho_2\cdots\rho_Q}\mathbf{\Gamma}^{L_f}(\vec{\rho}_1)$$
$$\times\mathbf{F}(\vec{\rho}_1\vec{\rho}_2)\cdots\mathbf{F}(\vec{\rho}_{N-1}\vec{\rho}_Q)\mathbf{\Gamma}^{00}(\vec{\rho}_Q). \tag{2}$$

For each i, j pair, $\mathbf{F}(\vec{\rho}_i\vec{\rho}_j)$ is a $(\lambda\times\lambda)$ matrix. Taken to the second order, $\lambda=6$. At second order, the RA method is convergent for most systems.[10] If the initial state in the photoexcitation has a high angular-momentum quantum number, then $\lambda=15$ (third order) or higher values may be required. In the following demonstration, we shall use $\lambda=6$. If higher values of λ are used, the time savings will increase linearly with λ. Using $\lambda=6$, $\mathbf{\Gamma}^{00}(\vec{\rho}_Q)$ is a (6×1) column vector while $\mathbf{\Gamma}^{L_f}(\vec{\rho}_1)$ is a (1×6) row vector. The scattering matrix $\mathbf{F}(\vec{\rho}_i\vec{\rho}_j)$ contains the temperature-correction factor $\mathbf{W}(\vec{\rho}_i\vec{\rho}_j)$, which is explicitly given in the work of Kaduwela, Friedman, and Fadley.[8] Direct evaluation of Eq. (1) requires a computation time that scales as n^{MS}. In the example given in this paper, to achieve convergence for a single Ni(001) layer, we need $n=253$ atoms and MS over 20. Thus, direct summing of Eq. (1) requires a computation time scaling as $(253)^{20}$, which obviously is impractical.

We shall cast Eq. (2) into a set of linear equations and obtain the solution by a relaxation-iterative method. To do this, we define a single-scattering propagator as

$$\mathbf{g}_{ij}=\frac{e^{i\rho_j}}{\rho_j}\mathbf{F}[k_0(\vec{R}_j-\vec{R}_i),k_0(\vec{R}_d-\vec{R}_j)]\mathbf{\Gamma}^{00}(\vec{\rho}_d)e^{-i\vec{k}_f\cdot\vec{R}_j}. \quad (3)$$

We notice that $\vec{R}_j$ is the last scattering before the electron propagates to the detector at $\vec{R}_d$. The phase factor $e^{-i\vec{k}_f\cdot\vec{R}_j}$ is added to account for the propagation with damping of the scattered electron from atom $\vec{R}_j$ towards the detector. This factor is not included in the RA formulation or the treatment of Kaduwela, Friedman, and Fadley[8] because they have assumed a real $\vec{k}_f$. Because there is inelastic damping inside the solid, $\vec{k}_f$ is a complex wave vector and its proper choice across the solid-vacuum interface has been discussed previously.[9,10] Since $\mathbf{\Gamma}^{00}(\vec{\rho}_d)$ is a (6×1) column vector, $\mathbf{g}_{ij}$ is also a (6×1) column vector. We represent the total propagator, after full multiple scattering as $\mathbf{G}_{ij}$, which is also a (6×1) column vector. In $\mathbf{G}_{ij}$ the electron undergoes many additional scattering events after leaving the atom at $\vec{R}_j$. If we write the separable scattering matrix as

$$\mathbf{F}_{ijl}=F[k_0(\vec{R}_j-\vec{R}_i),k_0(\vec{R}_l-\vec{R}_j)]\frac{e^{ik_0|\vec{R}_j-\vec{R}_i|}}{k_0|\vec{R}_j-\vec{R}_i|}$$

$$=F_{ij,kl}\delta_{jk}, \quad (4)$$

then, we can solve for $\mathbf{G}_{ij}$ by the following set of linear equations:

$$\sum_{k,l}\{\delta_{ik}\delta_{jl}\mathbf{I}-\delta_{jk}\mathbf{F}_{ij,kl}\}\mathbf{G}_{kl}=\mathbf{g}_{ij}. \quad (5)$$

Equation (5) is one of the principal results of this paper. Once the total propagator $\mathbf{G}_{ij}$ are calculated, the photoelectron-diffraction intensity for an emitter located at $\vec{R}_i$ is given by

$$I(\vec{k})\propto\left|\sum_{L_f}m_{L_f}e^{i\delta_{l_f}}\left(\mathbf{\Gamma}^{00}(\vec{\rho}_d)\mathbf{\Gamma}^{L_f}(\vec{\rho}_d)e^{-ik_f\cdot\vec{R}_0}+\sum_{j\neq i}\mathbf{\Gamma}^{L_f}(\vec{\rho}_j)\mathbf{G}_{ij}\right)\right|^2. \quad (6)$$

For given i, j, and l, the quantity $\mathbf{F}_{ij,kl}$, is a (6×6) matrix, $\mathbf{G}_{kl}$ and $\mathbf{g}_{ij}$ are (6×1) column vectors. Thus, Eq. (5) is of the familiar form $\{\mathbf{I}-\mathbf{M}\}\mathbf{x}=\mathbf{y}$. As indicated earlier, the exact solution of Eq. (5) requires calculating $\mathbf{x}=\{\mathbf{I}-\mathbf{M}\}^{-1}\mathbf{y}$ and the computation time scales as N^3, where $N=6n^2$. A faster way is to solve Eq. (5) by iteration as follows:

$$\mathbf{x}^{m+1}=\mathbf{M}\mathbf{x}^m+\mathbf{y}. \quad (7)$$

Equation (7) is equivalent to expanding $\{\mathbf{I}-\mathbf{M}\}^{-1}$ in a power series, i.e.,

$$\mathbf{x}=(\mathbf{I}+\mathbf{M}+\mathbf{M}\cdot\mathbf{M}+\cdots)\mathbf{y}. \quad (8)$$

The expansion in Eq. (8) converges if and only if the magnitude of the largest eigenvalue of $\mathbf{M}$, $|\lambda_M|$, is less than unit. Otherwise, Eq. (8) will diverge and produce unphysical results. However, it is possible to stabilize the iteration by introducing two adjustments to the scheme.

(1) For the vector $\mathbf{x}^{m+1}$, the latest values x_i^{m+1} for $1\leqslant i\leqslant j$ are used for calculating the element x_{j+1}^{m+1}. By using the latest values x_i^{m+1}, the right-hand side of Eq. (7) becomes closer to the current value and this makes the iteration more stable. This step has the additional advantage that it does not require the simultaneous storage of $\mathbf{x}^{m+1}$ and $\mathbf{x}^m$ as is necessary if Eq. (7) is solved by conventional iteration.

(2) The second adjustment is to include a relaxation parameter ω such that we write

$$x_i^{m+1}=\omega\tilde{x}_i^{m+1}+(1-\omega)x_i^m. \quad (9)$$

In Eq. (9), $\tilde{x}_i^{m+1}$ is the $(m+1)$th iteration obtained by using step 1. If $0<\omega<1$, we see that step 2 mixes ω and $(1-\omega)$ portions of the mth and $(m+1)$th iteration results to make up the new value. A choice of ω between 0.5 and 0.9 makes the iteration method convergent for all the materials tested, using a typical inelastic damping of 4 eV at $T=0$ K.

To demonstrate the relaxation-iterative (RI) method applied to clusters, we show in Fig. 1 the normalized photoelectron-diffraction spectra $[\chi=(I-I_0)/I_0]$ calculated for 49, 81, and 253 atom clusters of Ni. The Ni atoms are arranged in a Ni(001) plane, with the emitting atom at the center of a circle. Along the [001] direction, the radius of the circle contains 4, 5, and 9 atoms, respectively (excluding the emitting atom) for each cluster size. We use the same dynamical inputs chosen in a previous study: i.e., $L_f=s$-wave, inelastic damping $=4$ eV, and inner potential and temperature are set to zero.[10] Figure 1, upper panel, shows the normal emission χ_{cluster} by solving Eq. (5) using the direct-expansion method, i.e., Eq. (8). We see that direct expansion of $\mathbf{M}$ diverges for a Ni(001) plane of 81 atoms or larger. For the 49 atom cluster, the calculation does not diverge. However, the cluster is too small for its result to agree with that of an infinitely extended Ni(001) plane, i.e., χ_{slab}. The curve χ_{slab} is calculated by the conventional slab method using the $\{\mathbf{I}-\mathbf{M}\}^{-1}\mathbf{y}$ approach. In Fig. 1, lower panel, we show the

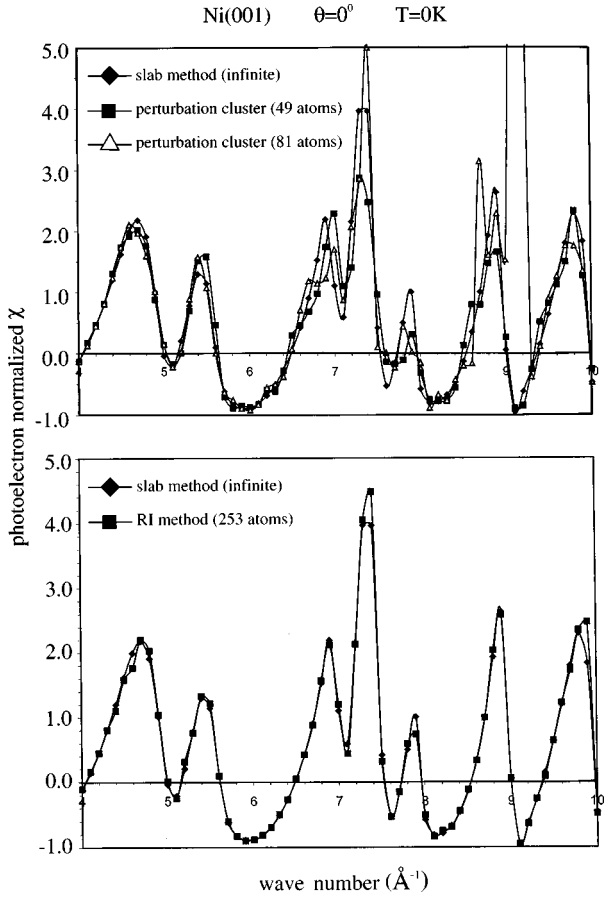

FIG. 1. Calculated normal-emission photoelectron-diffraction spectra for a single Ni(001) layer comparing the slab result (solid diamonds) with (i) upper panel: separable-representation perturbation-expansion calculations using 49 atoms (solid squares) and 81 atoms (hollow triangles). The 81-atom calculation shows divergence of the perturbation expansion. (ii) Lower panel: The same slab result compared to the separable-representation relaxation-iteration calculation of 253 atoms (solid squares), showing convergence of the two methods.

χ_{cluster} calculated by the RI method, i.e., step 1 and Eq. (9), for a 253-atom cluster. The relaxation factor ω is chosen as 0.8. There are three significant results to note: (i) For the 253-atom cluster, χ_{cluster} agrees well with χ_{slab}, (ii) the RI method is convergent, and (iii) in the separable representation, the computation time for the RI method scales only as $N^{1.5}$, while the $\{\mathbf{I}-\mathbf{M}\}^{-1}\mathbf{y}$ method scales as N^3. In order to calculate χ_{slab}, it is necessary to assume a long-range order in the Ni(001) plane. This reduces the slab system to one atom per unit cell. On the other hand, χ_{cluster} is calculated by the RI method with no requirement of order in the Ni plane.

It is easy to see why the RI method scales only as $N^{1.5}$. The iterative solution of Eq. (5) is

$$\tilde{G}_{ij}^{m+1}=\sum_l F_{ijl}G_{jl}^{m*}+g_{ij}, \tag{10}$$

where we use the latest values in G_{jl}^{m*}. Thus, $m*$ can be either the mth or $(m+1)$th order. Since the indices (i, j, and l) denote atomic sites, the computation of Eq. (10) scales as $n^3 \propto N^{1.5}$ because $N=6n^2$. On the other hand, the conventional solution of Eq. (5) by Gaussian substitution scales as N^3, even though there are many zeros in the left-hand side matrix of Eq. (5).

We show elsewhere that the backward-summing method introduced earlier[11] has the same convergence condition as direct expansion, i.e., Eq. (8). Therefore, the backward-summing method also diverges for a Ni(001) plane of 81 atoms under the same conditions. Steps 1 and 2 of the RI method modifies the expansion matrix $\mathbf{M}$ to a new expansion matrix:

$$\mathbf{M}'=(\mathbf{I}-\omega\mathbf{L})^{-1}\{(1-\omega)\mathbf{I}+\omega\mathbf{U}\}, \tag{11}$$

where $\mathbf{L}$, $\mathbf{U}$, and $\mathbf{I}$ are $(N\times N)$ matrices containing, respectively, the lower, upper, and diagonal elements of the matrix $\mathbf{M}$. We show elsewhere by choosing $0<\omega<1$, the largest eigenvalue of $\mathbf{M}'$ is less than unity even when $|\lambda_M|>1$. This is why the RI method converges for systems wherein the direct iteration diverges.

So far, we have applied the RI method to the separable representation cluster calculation. However, the RI method can equally be applied to nonseparable slab calculations for systems with long range order. The computation time scales as n^2, i.e., the number of atoms per unit cells. Thus, the RI method is best suited for supercell slab calculations. For example, in dynamical LEED calculations, the total T-matrix for layer i within a composite layer is given by

$$\sum_j \{\delta_{ij}\mathbf{I}-\tau_i\mathbf{G}_{ij}\}\mathbf{T}_j(\vec{k}j)=\tau_i(\vec{k}). \tag{12}$$

For given i, j, $\tau_i(\vec{k})$ and $\mathbf{T}_i(\vec{k})$ are column vectors of length $L=(l_{\max}+1)^2$ while $\tau_{i,LL'}$ and $\mathbf{G}_{ij,LL'}$ are $(L\times L)$ square matrices. Their definitions are found in standard LEED papers.[2] Since Eq. (12) again has the form $\{\mathbf{I}-\mathbf{M}\}\mathbf{x}=\mathbf{y}$ with dimension $N=n(l_{\max}+1)^2$, we can apply the RI method to solve for $\mathbf{T}_j(\vec{k})$. Here, n is the number of atoms per unit cell. In Fig. 2, we show IV curves calculated by the RI method compared to those using the conventional matrix-inversion method for the $c(2\times2)$ Au on Cu(001) system. We have included two rumpled $c(2\times2)$ Au-Cu alloy layers on top of eight (1×1) Cu layers, thus i or j runs over 12 subplanes in Eq. (12). We choose the same dynamical inputs as those used in a previous structural determination:[12] inelastic damping $=4.25$ eV, ten partial waves, inner potential $=10$ eV, and temperature correction for $T=300$ K is included. The relaxation factor $\omega=0.5$. In Fig. 2, the relaxation iteration is stopped at an accuracy of

$$\epsilon=\max\left|\sum_j (1-M)_{ij}x_j-y_i\right|\leq 5\times10^{-3}. \tag{13}$$

If we decrease ϵ to $\leq 1\times10^{-3}$, the IV curves calculated by the RI method becomes visually indistinguishable from those of the n^3-scaling matrix-inversion method.

Besides the two systems presented here, we have also tested other strong as well as weak scattering systems, e.g., Pt(001), disordered B-Si(111), etc. In each case, the RI method is numerically convergent to the ''exact'' result with a typical inelastic damping of 4 eV and without temperature correction (temperature correction further improves the convergence). The relaxation factor ω is usually between 0.5–0.9. The number of iterations required to reach convergence

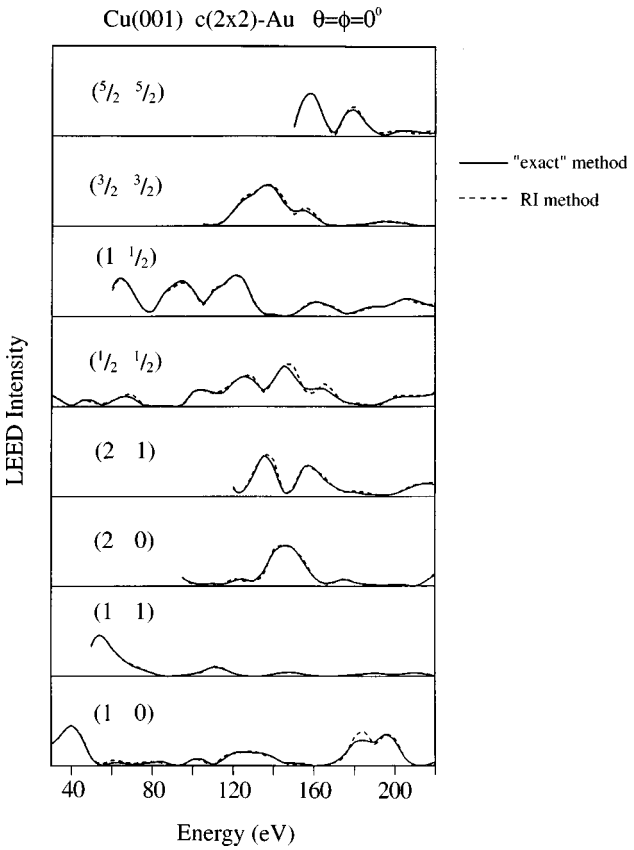

FIG. 2. Calculated LEED IV spectra for Cu(001) $c(2\times2)$ Au comparing results of slab-type Gaussian substitution method (solid lines) and the nonseparable relaxation-iterative method (dotted lines). The results show good convergence of the two methods.

is related to the MS order, the latter is typically between 15–30, depending on the magnitudes of damping and temperature correction. A systematic application of the RI method to different metal and semiconductor materials will be presented elsewhere. The RI method is well suited for solving the system of linear equations because $\mathbf{G}_{ij}$ or $\mathbf{F}_{ik,kl}$ decreases rapidly as the atomic separation $k_0|\vec{R}_j-\vec{R}_i|$ becomes large. Thus, while the dimension of the **M** matrix is large, there are many small elements (compared to unity) corresponding to large $(j-i)$ distances.

It is important to recognize that the reduction in the scaling from N^3 to N^2 (nonseparable representation) or $N^{1.5}$ (separable representation) is frequently a deciding factor whether a calculation is practical or not. For example, with the 253 atom cluster shown in Fig. 1, $N=2.53\times10^4$ in the nonseparable form (using ten partial waves). In the separable form, $N=3.84\times10^5$ using (6×6) matrices. To handle such large matrices by inversion is not practical in real applications. On the other hand, the 253-atom cluster calculation using the RI method is easily handled on an IBM RS6000 workstation. Equally important to stress is the fact that, as shown in Fig. 1, lower panel, and Fig. 2, the RI method is as accurate as the ''exact'' method.

The choice of using either the nonseparable or separable form depends on the number of atoms involved, the number of partial waves needed in the nonseparable form, and the dimension of the RA scattering matrix in the separable form. If we take typical values of ten partial waves and 6×6 RA matrices, then the respective computational times for the nonseparable and separable forms scale as 10^4n^2 and $36n^3$, where n is the number of atoms. Therefore, if n is 277 or less, then the separable form is faster, but if n is bigger than 277, the nonseparable form is faster. However, in either representation, the RI method is faster than the conventional Gaussian substitutional method by close to an order of N.

In conclusion, we have introduced a RI method for solving the Rehr-Albers separable-cluster problem and the conventional slab matrix-inversion problem. The method has been tested to be convergent for common systems of interest in either the separable form or the nonseparable form. With substantial savings in computation time and at no loss of numerical accuracy, the method is useful in future applications of multiple-scattering theories, particularly for systems where no long-range order is present.

This work was supported in part by HK RGC, HK RGC Central Allocation Vote, HKU CRCG, DOE Grant No. DE-FG02-84ER45076, and NSF Grant No. DMR-9214054.

[1] J. B. Pendry, *Low Energy Electron Diffraction* (Academic, London, 1974).
[2] M. A. Van Hove and S. Y. Tong, *Surface Crystallography by LEED* (Springer, Berlin, 1979).
[3] S. Y. Tong, H. Huang, C. M. Wei, W. E. Packard, F. K. Men, G. Glander, and M. B. Webb, J. Vac. Sci. Technol. A **6**, 615 (1988).
[4] M. Henzler, Surf. Rev. Lett. **4**, 481 (1997).
[5] C. S. Lent and P. I. Cohen, Surf. Sci. **139**, 121 (1984).
[6] J. J. Rehr and R. C. Albers, Phys. Rev. B **41**, 8139 (1990).
[7] See, for example, F. B. Hildebrand, *Introduction to Numerical Analysis* (McGraw-Hill, New York, 1956).
[8] A. P. Kaduwela, D. J. Friedman, and C. S. Fadley, J. Electron Spectrosc. Relat. Phenom. **47**, 223 (1991).
[9] S. Y. Tong and H. C. Poon, Phys. Rev. B **37**, 2884 (1988).
[10] Huasheng Wu, C. Y. Ng, T. P. Chen, and S. Y. Tong, Phys. Rev. B **57**, 15 476 (1998).
[11] Huasheng Wu, Yufeng Chen, D. A. Shirley, and Z. Hussian (unpublished).
[12] J. B. Tobin, G. D. Waddill, Hua Li, and S. Y. Tong, Phys. Rev. Lett. **70**, 4150 (1993).